UNIVERSITY OF CALIFORNIA SAN DIEGO

Organizing ES Induced Axonal Regeneration in Peripheral Nerve Injury

A Thesis submitted in partial satisfaction of the requirements
for the degree Master of Science

in

Bioengineering

by

Benjamin Francis Dela Cruz

Committee in charge:

Professor Yacov Koffler, Chair
Professor Adam J Engler, Co-Chair
Professor Alyssa Taylor

2026

The Thesis of Benjamin Francis Dela Cruz is approved, and it is acceptable in quality and form for publication on microfilm and electronically.

University of California San Diego

2026

DEDICATION

To my parents who have constantly been a stable backbone through all the difficulties in life. To my friends Rohan, Seuki, Eric, Carol and Beatriz who have been supportive of my education. Thank you for being supportive throughout my graduate and undergraduate careers.

TABLE OF CONTENTS

LIST OF FIGURES

LIST OF TABLES

LIST OF ABBREVIATIONS

BDNF	Brain Derived Neurotrophic Factor
cAMP	cyclic Adenosine Monophosphate
CNS	Central Nervous System
ES	Electrical Stimulation
GAP-43	Growth Associated Protein-43
Gel-MA	Gelatin Methacrylate
LAP	Lithium phenyl-2,4,6-trimethylbenzophosphinate
NGC	Neural Guidance Conduit/Scaffold
NGF	Nerve Growth Factor
PCL	Polycaprolactone
PEGDA	Polyethylene Glycol Diacrylate
PFA	Paraformaldehyde
PNI	Peripheral Nerve Injury
PNS	Peripheral Nervous System

ACKNOWLEDGEMENTS

Thank you to my family, friends and the Koffler and Tuszynski Labs for being a guide through my academic journey in graduate school.

I would like to specifically thank Dr. Jacob Koffler for being extremely patient while guiding me through this undertaking, his thoughtful insights on the scientific process, and his commitment to being a mentor. His instruction has given me the confidence to pursue future scientific and academic challenges.

I also would like to sincerely thank Alec Selcedo, and Isac Lazarovits, for being a reliable source of support, for their guidance, and feedback through this project. I would also like to express my thanks to Maryam Mansoor for making the laboratory experience fun and for her constant belief and encouragement as I developed this project.

Finally, I would like to express my gratitude to the University of California, San Diego Gene Lay Department of Bioengineering for granting me the opportunity to conduct research in an environment filled with a diverse field of research areas in which we can explore many avenues. Researching at UCSD has been a defining moment in my academic and professional career.

VITA

2024 Bachelor of Science in Bioengineering, University of California, Riverside

2026 Master of Science in Bioengineering, University of California, San Diego

PUBLICATIONS

Okoro, P. D., Dalsania, K., Iragavarapu, S. B., Dela Cruz, B., Banerjee, A., Basarabienk, M., Haase, M. F., Anvari, B., & Noshadi, I. (2025). Bicontinuous microarchitected scaffolds provide topographic cues that govern neuronal behavior and maturation. *Advanced Functional Materials, 36*(5), e09452. https://doi.org/10.1002/adfm.202509452

ABSTRACT OF THE THESIS

Organizing ES Induced Axonal Regeneration in Peripheral Nerve Injury

by

Benjamin Francis Dela Cruz

Master of Science in Bioengineering

University of California San Diego, 2026

Professor Yacov Koffler, Chair
Professor Adam Engler, Co-Chair

Brief electrical stimulation (ES) following peripheral nerve repair has emerged as a promising strategy to accelerate axonal regeneration; however, ES may reduce regenerative specificity by increasing axonal mistargeting and inappropriate motor neuron reinnervation. Biomimetic multichannel scaffolds that recapitulate peripheral nerve fascicular architecture provide structural guidance for organized axonal regeneration and may improve the efficacy of ES. This study evaluated whether combining brief ES with a biomimetic multichannel scaffold enhances regeneration following peripheral nerve injury. Thirty-six Fischer 344 rats underwent 1-

cm sciatic nerve transection and biomimetic multichannel scaffold implantation. Eighteen animals received intraoperative ES of the proximal nerve stump (6 V, 20 Hz, 110 μs pulses for 10 min). Samples were collected at 1, 3, and 5 weeks for histological and functional analyses. Axons within the proximal nerve, scaffold, and distal nerve were quantified, and gastrocnemius muscle weight was measured as an indicator of target muscle reinnervation. ES significantly increased axonal regeneration within the scaffold at week 1 (124 ± 31 vs. 38 ± 5 axons; $p = 0.0141$). At week 3, scaffold + ES significantly increased distal nerve axons (117 ± 21 vs. 19 ± 4; $p = 0.0010$). At week 5, ES treated animals had greater gastrocnemius muscle weight (0.332 ± 0.010 vs. 0.273 ± 0.015 g; $p = 0.0155$). These findings demonstrate a temporal progression of enhanced regeneration following combined ES and biomimetic multichannel scaffold implantation, with early axonal growth, subsequent distal nerve regeneration, and improved target muscle retention.

INTRODUCTION

Despite recent advances, peripheral nerve injuries (PNI) remain a significant clinical challenge in the field of neuroscience. PNI predominantly affects young, otherwise healthy individuals, with 83% of patients under the age of 55, and has roughly equal prevalence between men and women [1]. Its consequences, including pain, spasticity, and in severe cases, loss of sensory and motor function, carry both physical and psychological costs. Most of these outcomes stem from poor axon reconnection between the proximal and distal nerve stumps. Although the peripheral nervous system retains some capacity for self-repair, regenerating at roughly 1–3 mm/day, gap injuries remain difficult to treat as axons that regrow without proper directional guidance frequently fail to reach and reinnervate their distal targets [2, 3].

Electrical stimulation (ES), the brief application of a low-voltage current directly to the nerve at the time of surgical repair, has been studied since the 1980s as a strategy to accelerate axonal regeneration following peripheral nerve injury. Currently, ES is being used as an aid in pain management and has had wide success in muscle preservation [4]. However, clinical application of direct nerve ES to enhance axonal regeneration has been limited. In vitro, ES reliably promotes axon outgrowth through an upregulation in cAMP and a release of BDNF and NGF to enhance axon repair [5]. In-vivo application of ES does increase axon regeneration, but it also results in a higher rate of misdirected regrowth of axons and the inappropriate reinnervation of unintended targets [6].

Open, single-lumen tube conduits is another approach used to enhance regeneration. This conduit is used to provide physical support to axons bridging the gap from the proximal to the

distal stump. However, their simple architecture offers no internal structure, and axons within frequently disperse and lose directionality before reaching the far end of the gap [7-9]. Advances in neural tissue engineering and biocompatible hydrogel 3-D printing have since enabled a more structured alternative in the development of biomimetic multichannel neural guidance conduits, or scaffolds (NGCs). Unlike open single-lumen tubes, NGCs contain an internal array of parallel microchannels that subdivide the conduit lumen, more closely approximating the fascicular architecture of a native nerve. This internal structure creates a supportive, compartmentalized microenvironment that bridges the lesion site while keeping regenerating axons aligned across the length of the gap. The microchannel approached has been tested in spinal cord injury and peripheral nerve injury. Animals treated with microchannel scaffolds showed improved functional recovery compared with controls [7, 8, 10].

Electrical stimulation of peripheral nerves delivered at the time of repair accelerates axonal regeneration, while multichannel NGCs improve the directionality of otherwise misaligned axons, yet the combined effect of these two approaches has been limited. Given their complementary mechanisms, an initial study evaluating ES together with a multichannel scaffold is warranted. In this study, we tested whether adding electrical stimulation to a multichannel neural guidance scaffold changes overall axon regrowth, the myelination state of Schwann cells, and downstream muscle reinnervation (measured as gastrocnemius muscle weight retention) relative to scaffold implantation alone.

BACKGROUND / LITERATURE REVIEW

Peripheral Nervous System Anatomy and Biology

The nervous system comprises the central nervous system (CNS) and the peripheral nervous system (PNS). The CNS, the brain and spinal cord, performs higher-order processing, decision-making, and integration of sensory input, and is correspondingly the most protected part of the nervous system. Because the CNS is enclosed and shielded from direct injury, communication with the rest of the body relies on the PNS, a separate network that carries sensory information and motor commands over long distances via action potentials. The PNS is made up of several cell types, but axons and Schwann cells are primarily responsible for rapid, long-distance signal transmission.

Peripheral nerve tissue is organized hierarchically (Figure 1). Individual axons are ensheathed by the endoneurium, groups of axons are bundled into fascicles enclosed by the perineurium, a semi-permeable layer that both protects the fascicle and allows nutrient exchange, and the entire nerve is encased by the epineurium, through which blood vessels travel to supply the tissue with oxygen and nutrients [11].

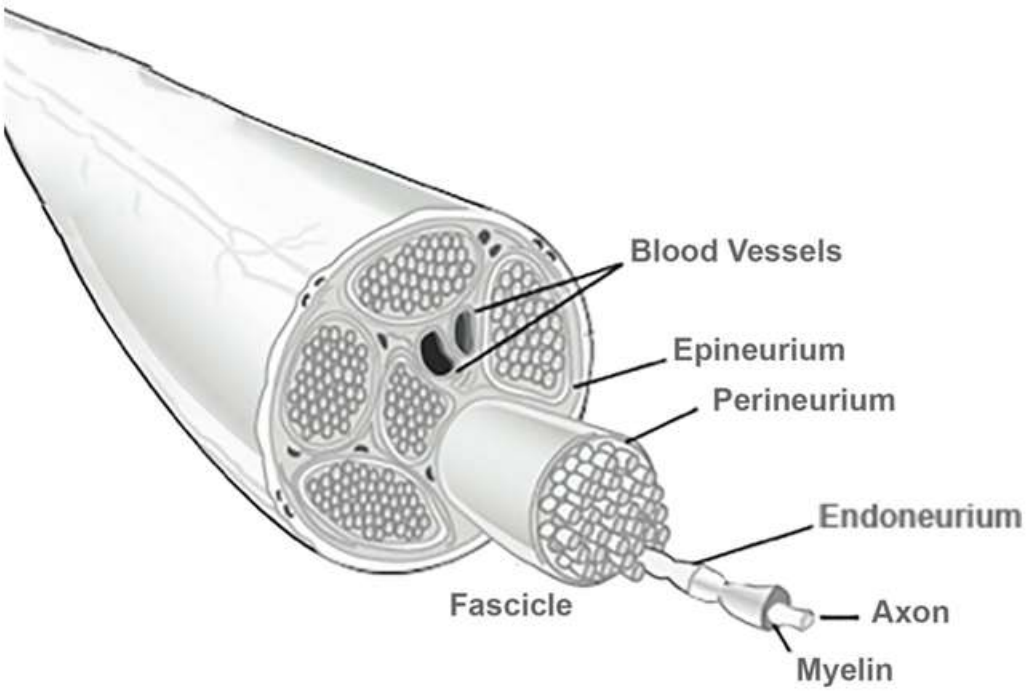

Figure 1: Peripheral nerve microstructure. The nerve is organized into multiple fascicles containing individually myelinated axons. Each axon is surrounded by the endoneurium, fascicles are enclosed by the perineurium, and the entire nerve is encased by the epineurium. Blood vessels traverse the epineurial space to supply oxygen and nutrients. This hierarchical organization provides structural support, mechanical protection, and a microenvironment essential for axon function and regeneration after injury. From Pedrosa, S. S., Caseiro, A. R., & Maurício, J. D. S. and A. C. (2017). Scaffolds for Peripheral Nerve Regeneration, the Importance of In Vitro and In Vivo Studies for the Development of Cell-Based Therapies and Biomaterials: State of the Art. In *Scaffolds in Tissue Engineering—Materials, Technologies and Clinical Applications*. IntechOpen. https://doi.org/10.5772/intechopen.69540.

Axons are long projections of neurons. Their main function is to conduct electrical impulses (action potentials) over long distances to downstream neuronal, muscular, or sensory targets, releasing neurotransmitters at the axon terminal [12]. Axon diameter typically ranges from 1 µm to 25 µm, and length ranges from millimeters up to roughly a meter, depending on function and location. Efficient signal conduction requires the action potential to propagate quickly along the axon with minimal signal loss. In the PNS, accelerated signal propagation is facilitated by Schwann cells through the formation of myelin sheaths.

Schwann cells are the principal glial cells of the PNS, responsible for myelinating, supporting, maintaining, and repairing axons [13]. Myelination is the formation of a lipid-rich

sheath around the axon, which increases conduction velocity, functioning much like an insulator [12, 14]. Myelin sheath formation along the axon is discontinuous, creating nodes of Ranvier. Employing the jump mechanism from one node of Ranvier to the next, electrical signal propagation becomes much faster down sheathed axons [13]. To support and maintain axons, Schwann cells also provide energy metabolites, shuttling them through monocarboxylate transporters available along the surface of the axon and inner membrane of the Schwann cell [14]. Schwann cells also have a degree of plasticity, capable of transitioning to a repair phenotype responsible for supporting axon regeneration depending on location and degree of axon damage [15].

Injury Mechanisms

Peripheral nerves lack the protective bony casing of the CNS and are especially vulnerable to injury in the extremities, where they run close to muscle and skin. Seddon's classification and further Sunderland's classification remain the standard framework for grading PNI severity, from mildest to most severe: neurapraxia, axonotmesis, and neurotmesis [16-18]. Table 1 summarizes the tissue-level damage and expected recovery for each grade.

Table 1: Classification of peripheral nerve injuries according to Sunderland and Seddon. Peripheral nerve injury severity is categorized using Sunderland's five-grade system alongside Seddon's classifications, with increasing grade corresponding to greater disruption of axonal and connective tissue structures and progressively reduced potential for spontaneous functional recovery.

Grade	Classification	Tissue damage	Typical recovery
1	Neurapraxia	Axon intact, conduction block, often with demyelination	Full recovery within days to weeks
2	Axonotmesis	Axon damaged, endoneurium intact	Recovery likely, endoneurial tube guides regeneration
3	Axonotmesis	Axon and endoneurium damaged; perineurium intact	Recovery possible, reduced relative to Grade 2
4	Axonotmesis	Axon and perineurium damaged; endoneurium intact	Reduced likelihood of spontaneous recovery
5	Neurotmesis	Complete transection of axon, endoneurium, and perineurium	Poor without surgical repair, no physical guide for regenerating axons

As injury grade increases from 2 to 4, the progressive loss of connective-tissue scaffolding reduces the likelihood of spontaneous, well directed regeneration. Neurotmesis (Grade 5), complete transection of the axon and all surrounding connective tissue, is the most severe injury type, because no physical guide remains to direct regenerating axons toward their original endoneurial tubes. Functional recovery after neurotmesis is generally poor even with surgical intervention, particularly in long gap injuries where the proximal and distal stumps cannot be directly reconnected.

Peripheral Nervous System Repair

Unlike the CNS, the PNS is capable of regeneration, a process involving three key stages: Wallerian degeneration, axonal regeneration, and end organ reinnervation. Combined, these

processes seek to clear all debris and rejoin the proximal and distal stumps of an injured nerve, culminating in the reestablishment of end-organ functionality.

Wallerian degeneration is a programmed response that occurs in the distal nerve after transection or crush injury. It is a highly active, coordinated clearance of myelin and axonal debris that transforms the nerve stump from a stable, signal conducting structure into an environment conducive to regeneration (Figure 2). In humans, at least 50% of affected axons complete Wallerian degeneration within 7 days of injury [19].

Degeneration begins at the injury site, where axons swell and fragment (Figure 2B). Loss of NMNAT2, an enzyme required for axon survival, allows nicotinamide mononucleotide (NMN) to accumulate to toxic levels. SARM1 activation then triggers energy failure and structural collapse of the axon [20]. Within 24–36 hours, the axonal cytoskeleton breaks down and Schwann cells begin clearing the surrounding myelin (Figure 2C). Macrophages subsequently infiltrate the exposed tissue to help clear axon and myelin debris (Figure 2D-E). Under ideal conditions, the endoneurial tubes remain intact, providing a path for axons and regenerative phenotype Schwann cells to realign from the proximal to the distal stump (Figure 2F-G).

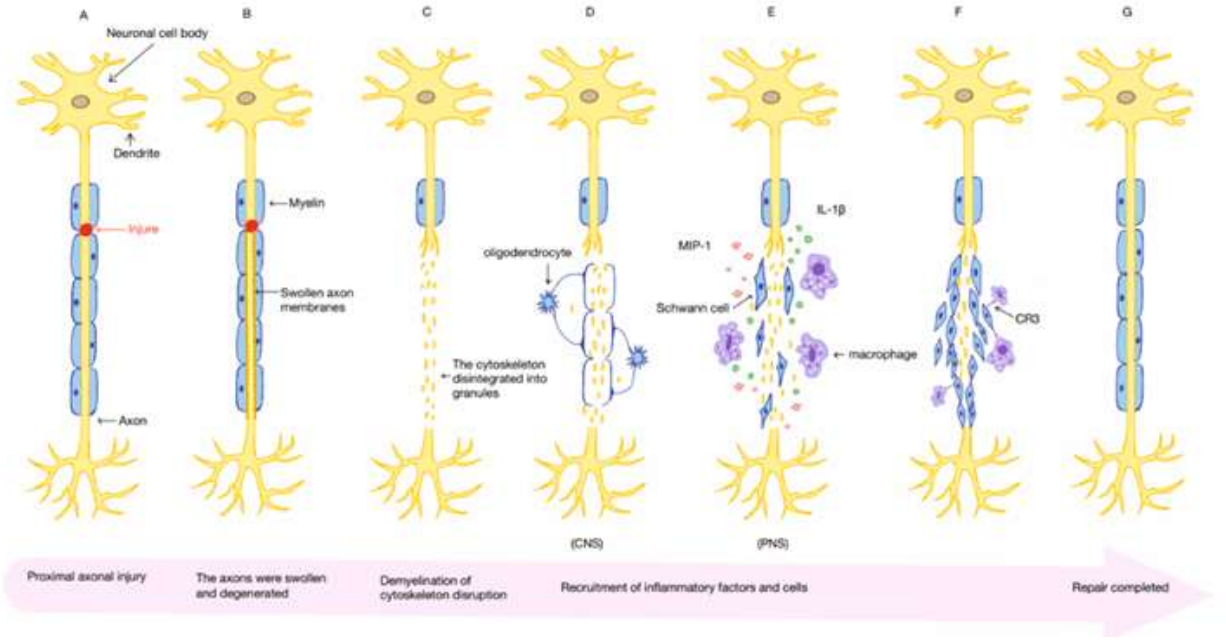

Figure 2: Wallerian degeneration and peripheral nerve regeneration following axonal injury. (A) Injury initiates degeneration distal to the injury site. (B) The injured axon swells and fragments. (C) Demyelination and cytoskeletal breakdown occur as the distal axon degenerates. (D) Inflammatory signaling recruits glial and immune cells; in the CNS, oligodendrocytes provide limited regenerative support. (E–F) In the PNS, Schwann cells, macrophages, and inflammatory mediators coordinate debris clearance and promote regeneration. (G) Regenerating axons are remyelinated by Schwann cells, restoring nerve structure and function. From Tian, R., Zhou, Y., Ren, Y., Zhang, Y., & Tang, W. (2025). Wallerian degeneration: From mechanism to disease to imaging. *Heliyon, 11*(1), e40729. https://doi.org/10.1016/j.heliyon.2024.e40729.

Toward the end of Wallerian degeneration, the remaining Schwann cells organize into Bands of Büngner, a morphological structure that forms natural conduits from the distal to the proximal stump, facilitating axonal reconnection. During this process, the proximal segment begins to reform. Growth cones assemble to rebuild nerve fibers through the injury site, signaled by an upregulation in GAP-43, a marker of axonal regeneration. These growth cones extend from the healthy proximal segment and seek out the distal Bands of Büngner, reestablishing axonal continuity and repairing the nerve. Processes of axon regeneration are controlled by an upregulation in related regeneration-associated genes (RAGs), and corresponding neurotrophic factors such as NGF, and BDNF [22, 23].

Gap defects can disrupt this process, allowing axons to grow without proper directionality. Left untreated, misdirected axons can infiltrate inappropriate tissue, causing pain, numbness, and loss of function. Prolonged denervation from axonal misalignment can also lead Schwann cells to undergo autophagy and eventual senescence or apoptosis [24], while the end organ itself atrophies over time, contributing to chronic sensory and motor dysfunction [25, 26].

Guidance and Combinatorial Approaches

Addressing incomplete regeneration in gap defects, particularly after loss of the endoneurial tube, has become more feasible with advances in biocompatible composite materials and fabrication methods [27-30]. These advances have driven research toward implantable conduit devices that bridge the defect and guide axons from the proximal to the distal stump, providing the structural and directional support long-gap injuries require.

The clinical gold standard for repairing peripheral nerve injury with a gap remains the autologous nerve graft, in which a segment of the patient's own nerve, typically harvested from the leg, is transplanted to the injury site, avoiding the risk of immunological rejection. However, donor site morbidity and chronic pain at the harvest site are common, and functional outcomes remain inconsistent, with fewer than 50% of patients recovering meaningful function [31-33]. These limitations have driven increasing interest in nerve guidance conduits (NGCs), or scaffolds, which aim to improve axon directionality while avoiding the complications associated with autograft repair.

NGC design follows four main considerations. Permeability to allow nutrient and oxygen diffusion into the regeneration site before vascularization and to support cellular migration into the

scaffold. Flexibility to avoid mechanical injury to surrounding tissue and regenerating axons, particularly across joints. Resistance to inappropriate swelling, which can block the conduit entrance and prevent regeneration. Finally, a degradation rate matched to the pace of repair [29]. In summary, an ideal conduit remains open as axons grow from the proximal stump toward the distal side, flexes with movement, stays patent for the duration of reinnervation, and degrades gradually without swelling the surrounding tissue.

Early conduit designs used a simple, open, single-lumen tube made from natural fibers such as collagen and chitosan, or synthetic polymers such as polyglycolic acid (PGA) or polycaprolactone (PCL) to provide a direct, uninterrupted connection between the proximal and distal stumps [27]. These open tubes, however, struggle to achieve point-to-point axon reconnection. Their relatively large diameter compromises structural integrity, offers little resistance to bending, and fails to constrain the direction of axonal regrowth, limiting their effectiveness to short gap rather than long gap injuries [32, 34].

Advances in biocompatible hydrogel polymers and microfabrication have since enabled multichannel conduits that add internal rigidity and directional guidance for regenerating axons. This architecture more closely mimics the fascicular pattern of native nerve tissue while preserving space for cellular regrowth [10, 30, 35]. By resembling the multiple basal lamina tubes (fascicles) of native nerve, multichannel NGCs appear to limit the axonal dispersion seen with single hollow tubes. Multichannel scaffolds have also demonstrated regenerative efficacy comparable to autograft in long-gap peripheral nerve defects [8]. Usage of biomimetic multichannel scaffolds serves to guide axons more effectively from the proximal to distal stump, increasing guidance and matching autograft performance, the current clinical standard in rat and rabbit models of sciatic nerve injury. In long-gap injuries, the directionality provided by a biomimetic multichannel

scaffold is a major stepping stone in finding a solution for gap rehabilitation. A combination of a secondary method to accelerate axon regrowth may further enhance axon regeneration and eventual propagation into the distal side of the injury.

Electrical stimulation application for nerve regeneration in proximal nerve

Electrical stimulation (ES) has been investigated as a strategy for promoting peripheral nerve regeneration for several decades. Early in vivo studies demonstrated that externally applied electrical currents could influence neuronal regeneration, building upon the established role of endogenous electrical activity in communication and function. Subsequent studies have demonstrated that ES can enhance axonal regeneration through several cellular mechanisms. Following PNI, ES can increase intracellular calcium concentrations and activate downstream signaling pathways, including cyclic adenosine monophosphate (cAMP) dependent pathways, that promote the expression of regeneration-associated genes (RAGs), axonal sprouting, and neuronal survival [36].

In addition to directly affecting neurons, ES can influence other cell types within the peripheral nerve that are critical for regeneration. Schwann cells, the principal glial support cells of the PNS, undergo phenotypic and morphological changes following nerve injury and play an important role in supporting axonal regeneration. In vitro studies have demonstrated that ES can alter Schwann cell morphology and enhance their ability to support neurite outgrowth. For example, it has been demonstrated that direct-current stimulation of Schwann cells altered cellular morphology and promoted sustained increases in neurite outgrowth [37]. The authors observed changes in Schwann cell alignment and morphology following stimulation, with the greatest

morphological responses occurring at intermediate stimulation intensities. ES has also been associated with changes in neurotrophic signaling, including increased production of nerve growth factor (NGF), which can further support axonal growth and regeneration [37]. These findings suggest that the regenerative effects of ES may extend beyond direct stimulation of neurons and may also involve modulation of the cellular environment surrounding regenerating axons. However, the effects of ES on Schwann cell behavior and neurotrophic signaling in vivo remain less well characterized and warrant further investigation.

The regenerative effects of ES have been demonstrated extensively in animal models of peripheral nerve injury. Brief ES applied following nerve injury has been shown to accelerate axonal regeneration and promote earlier reinnervation of target tissues [36, 38]. More recent work has demonstrated in a rat femoral nerve model that continuous low-frequency ES applied to the proximal nerve stump accelerated the progression of regenerating axons toward the target muscle, reducing the period from 10 weeks to 3 weeks [39]. ES is thought to act, in part, through activity dependent signaling involving cAMP, which promotes axonal sprouting and neuronal regenerative responses [36, 40]. In vitro studies have similarly demonstrated that manipulation of cAMP signaling can promote neurite outgrowth and extension in cultured motoneurons, further supporting the importance of activity-dependent intracellular signaling in axonal regeneration [41]. Together, these findings demonstrate that ES can influence both the rate and extent of axonal regeneration following peripheral nerve injury.

Importantly, the regenerative effects of brief ES observed in animal models have also demonstrated translational potential in human peripheral nerve repair. Clinical studies investigating postoperative ES following peripheral nerve decompression and repair have reported improvements in measures of motor axon regeneration and functional recovery [42]. These

findings suggest that ES can be applied in a clinically feasible setting and may provide regenerative benefits beyond those observed solely in experimental animal models. However, the clinical application of ES for gap peripheral nerve injuries remains less established, particularly when ES is combined with a structural nerve guidance strategy.

The parameters used to administer ES vary considerably across studies, including stimulation duration, voltage, frequency, and pulse width. Among these parameters, stimulation frequency and duration have received considerable attention in studies of peripheral nerve regeneration. Low frequency stimulation, particularly at approximately 20 Hz, has repeatedly demonstrated regenerative effects in animal models [36, 43]. Early studies commonly used a 60-minute stimulation period as a brief ES protocol, while more recent studies have investigated shorter stimulation durations. Roh et. al [39] demonstrated that short duration 10-minute, pulsatile ES was sufficient to accelerate axonal regeneration and functional recovery following tibial nerve injury and repair in rats, providing further evidence that prolonged stimulation may not be necessary to achieve regenerative effects. The ability to achieve regenerative effects using shorter stimulation periods is particularly relevant for clinical translation because reducing stimulation duration may improve the practicality of incorporating ES into postoperative treatment protocols. Similarly, pulse widths on the order of approximately 100–300 μs have been used in peripheral nerve stimulation studies, although the optimal combination of stimulation parameters remains incompletely defined [4, 6, 38].

Despite its ability to accelerate axonal regeneration, ES alone may not address the structural challenges associated with long-gap peripheral nerve injuries. ES provides a biological stimulus that promotes axonal growth however, it does not inherently provide directional guidance for regenerating axons as they traverse the site of injury [44, 45]. This distinction is particularly

important in long-gap injuries, where regenerating axons must travel a substantial distance before reaching the distal nerve stump. Furthermore, prolonged denervation results in progressive changes within the distal nerve and Schwann cell population that reduce the regenerative capacity of the distal environment [24]. Therefore, accelerating axonal growth alone may not be sufficient to achieve effective reconnection with the distal nerve and subsequent end-organ reinnervation.

The combination of ES with a structural guidance strategy may therefore provide a complementary approach to peripheral nerve repair. While ES can provide a biological stimulus to promote and accelerate axonal regeneration, a multichannel nerve guidance scaffold can provide physical organization and directional guidance as regenerating axons traverse the injury site. Combining these approaches may allow the regenerative benefits of ES to be paired with the organizational benefits of a structured scaffold, potentially improving the progression of axons across a long-gap injury while promoting more directed regeneration toward the distal nerve.

Based on this rationale, the present study utilized a short duration ES protocol in combination with a multichannel nerve guidance scaffold.

A stimulation protocol consisting of 6 V, 20 Hz, 110 μs pulses for 10 minutes was selected based on previous literature demonstrating regenerative effects associated with low-frequency and short-duration ES [1, 38, 39, 43]. The use of a 20 Hz stimulation frequency and 110 μs pulse width was informed by parameters previously investigated in peripheral nerve regeneration studies, while the 10-minute stimulation duration was selected to provide a shorter and potentially more clinically practical intervention compared with the historically utilized 60-minute protocols. The demonstration that short-duration, pulsatile ES can accelerate regeneration following peripheral nerve repair further supports the use of a brief stimulation paradigm [39]. This approach was

intended to determine whether the addition of brief ES to a multichannel scaffold could enhance the progression of axonal regeneration across the injury over time.

Summary

Peripheral nerve injury is classified into three broad categories of increasing severity, with complete nerve transection, neurotmesis being the most severe. The clinical gold standard for repair, the autograft, relocates healthy nerve from a second site in the same patient, requiring an additional surgical site and, in large-gap injuries, sacrificing function at the donor site. Nerve guidance conduits have been explored as an alternative. Early open tube designs showed disordered, low efficiency regeneration compared with autograft, while more recent biomimetic multichannel scaffolds have demonstrated regenerative efficacy comparable to autograft implantation. In parallel, electrical stimulation of the proximal nerve has long been shown to increase axonal regeneration, but ES alone does not reliably reconnect axons across a gap injury. Combining these two approaches may address the limitations of each used in isolation.

Rationale

Despite advances in both NGC architecture and ES, the interaction between the implantation of physical guidance multichannel NGCs and the biological effects of applied brief electrical stimulation remains incompletely understood. In particular, little is known about how ES influences the temporal progression of axonal regeneration through a biomimetic multichannel scaffold and its subsequent extension into the distal nerve.

A multichannel NGC provides structural guidance for regenerating axons, while ES provides an additional biological stimulus to promote regeneration; combining the two may address limitations inherent to each strategy used alone. This study investigates whether electrical stimulation changes the progression of axonal regeneration through a biomimetic multichannel NGC into the distal nerve, and its effect on end-organ (muscle) retention, following sciatic nerve transection.

We hypothesized that adding electrical stimulation to a biomimetic multichannel scaffold would have a pro-regenerative effect on axonal regrowth, increasing total axons over time relative to scaffold alone, decreasing end-organ degeneration, and potentially affecting Schwann cell presence across all injury phases. The specific aim of this study was to determine the efficacy of combining electrical stimulation with a multichannel NGC relative to scaffold implantation alone.

METHODOLOGY

This study used a rat sciatic nerve transection model to compare axonal regeneration and end-organ retention between two treatment groups: multichannel scaffold implantation alone, and multichannel scaffold implantation combined with electrical stimulation (ES). Figure 3 summarizes the overall experimental design, including the injury model, scaffold composition, treatment groups, and tissue collection timeline.

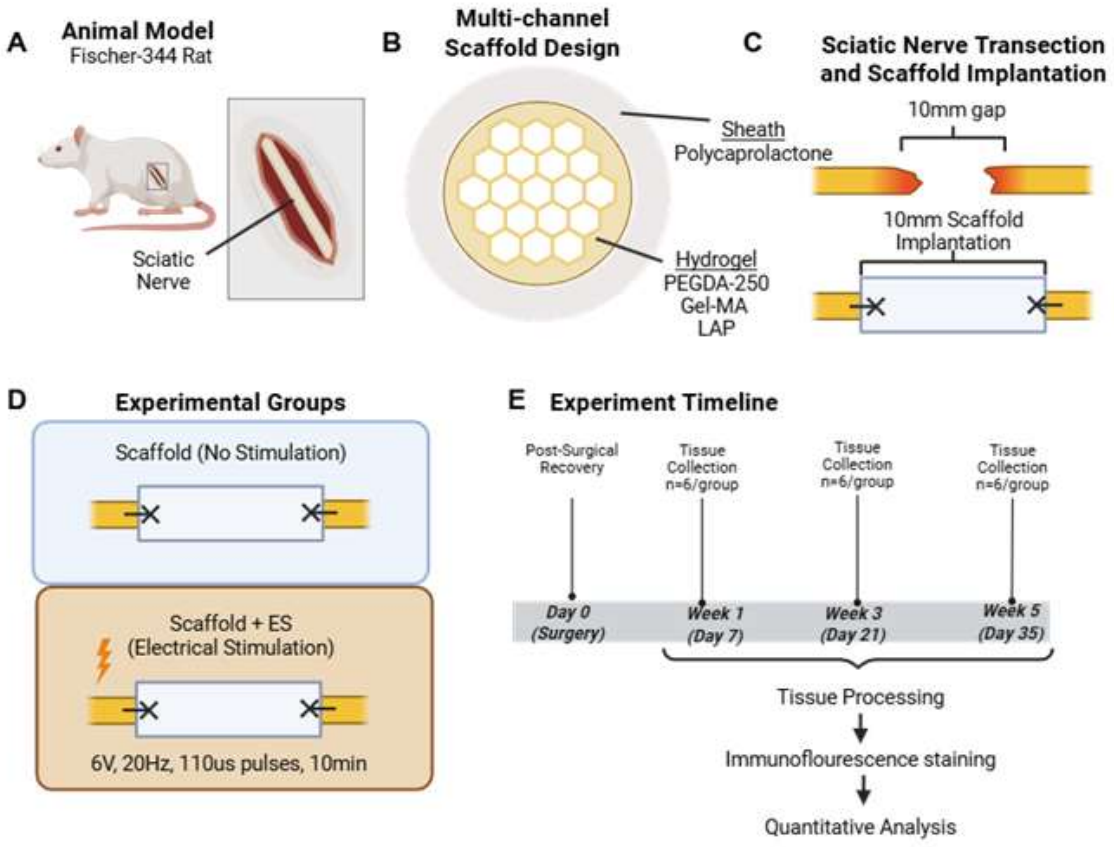

Figure 3: Experimental design for evaluation of tissue-engineered scaffolds in a rat sciatic nerve injury model. (A) Adult Fischer-344 rats underwent sciatic nerve transection to create a 10-mm nerve gap. (B) Schematic of the multichannel scaffold, consisting of a polycaprolactone (PCL) sheath surrounding a PEGDA-250/GelMA hydrogel containing lithium phenyl-2,4,6-trimethylbenzoylphosphinate (LAP) photoinitiator. (C) A 10-mm scaffold was implanted to bridge the 10-mm sciatic nerve defect. (D) Animals were assigned to scaffold-only or scaffold+ES treatment groups. ES consisted of 6 V, 20 Hz stimulation with a 110 µs pulse width for 10 minutes. (E) Experimental timeline: surgery (Day 0), tissue collection at 1, 3, and 5 weeks post-implantation (Days 7, 21, and 35), followed by tissue processing, immunofluorescence staining, and quantitative analysis.

Neural Guidance Conduit/ Scaffold Formulation

Neural guidance conduits (NGCs) were fabricated from a gelatin-based hydrogel solution consisting of 7.5% gelatin methacrylate (GelMA), 25% polyethylene glycol diacrylate (PEGDA), and 2% lithium phenyl-2,4,6-trimethylbenzoylphosphinate (LAP) photoinitiator (Figure 3B). This photopolymerizable solution was printed on a digital light processing (DLP) printer capable of producing millimeter-scale constructs. All animals received an NGC of uniform design, consisting of a 10 mm-long, 2 mm-wide hydrogel construct containing 19 parallel 0.2 mm-diameter channels running the full length of the scaffold. A polycaprolactone (PCL) sheath was placed around each NGC to facilitate suturing during implantation.

Surgical Implantation and Electrical Stimulation

The animal model was the Fischer-344 rat, with left sciatic nerve transection followed by NGC implantation at the injury site (Figure 3A). Subjects were divided into two treatment groups (n = 18 per group): multichannel NGC implantation alone, and NGC implantation with electrical stimulation. Each group was further divided into three time points week 1, week 3, and week 5 (n = 6 per time point).

All surgeries used wildtype, female Fischer-344 rats weighing 160–180 g and aged 2–4 months. Animals were anesthetized with a ketamine/xylazine cocktail (100 mg/mL, administered at 0.1 mL/100 g body weight) and received TOBREX eye drops to prevent corneal drying. The surgical site was shaved from the mid-back to the left foot. An incision was made from the top of the adductor longus through the vastus medialis to expose the sciatic nerve, which was then transected to create a 10 mm gap simulating a full transection injury. The NGC was implanted

immediately following transection (Figure 3C). In the ES group, stimulation was delivered to the nerve proximal to the injury site using an A-M Systems Model 3820 Multistim Stimulus Isolator (AC biphasic, 6 V, 20 Hz, 110 μs pulse width, applied for 10 minutes) (Figure 3D).

The incision was closed with interrupted sutures and wound clips, and bupivacaine coagulating powder was applied to support wound closure before anesthesia was reversed. Animals received meloxicam for post-surgical analgesia and were monitored daily for the first 10 days (with additional BAR checks for the first three days), then weekly until the scheduled collection date. Animals in the week 1 cohort were collected on day 7, as specified by the study parameters. All procedures followed IACUC approved protocols for humane animal care.

Histology and Immunohistochemistry

Tissue was collected following deep anesthesia with a triple anesthetic cocktail (ketamine 150 mg/kg, xylazine 7.2 mg/kg, acepromazine 1.5 mg/kg). A bilateral incision below the xiphoid process exposed the chest cavity, and a needle inserted into the aortic arch was used to perform saline perfusion followed by fixation with 4% paraformaldehyde (PFA). Gastrocnemius muscles were isolated and weighed, and the scaffold together with adjacent proximal and distal nerve segments was isolated and post-fixed in 4% PFA for 24 hours, followed by cryoprotection in 30% sucrose for 5 days.

After sucrose immersion, nerve segments were embedded in OCT compound and cryosectioned at 35 μm using a Leica CM1950 cryostat. Sections were mounted on microscope slides for immunohistochemistry.

Immunohistochemical staining was carried out over 5 days. Day 1: sections were washed 3× in TBS, treated with 5% Proteinase K for 20 minutes, blocked in 5% normal donkey serum (NDS) in TBS-T, and incubated with primary antibodies (1:500) for 3 days. Day 4: sections were washed 1× in TBS, stained with DAPI for 5 minutes, washed 2× in TBS, and incubated with secondary antibodies (1:250), Donkey Anti-Mouse (488) and Donkey Anti-Rabbit (568) for 24 hours. Day 5: sections received a final 3× TBS wash and were coverslipped with 200 µL Mowiol, then left to cure for 2 days before imaging.

Regenerating axons were visualized using SMI-312 (BioLegend, 837904), a pan-axonal marker recognizing phosphorylated neurofilament proteins. SMI-312 is a mixture of monoclonal antibodies that together label a complex network of axons, binding heavily phosphorylated epitopes on NF-H (200–220 kDa), NF-M (145–160 kDa), and NF-L (68–70 kDa) [46]. Neurofilament expression is one of the earliest recognizable features of the maturing nervous system and correlates with axon diameter, which in turn influences conduction velocity [47]. Increased SMI-312 labeling in a regenerating nerve therefore reflects increased axonal presence. Schwann cell myelination and overall Schwann cell presence were assessed using S100B (Invitrogen, PA5-78161), a broad Schwann cell marker that labels the S100B calcium-binding protein on the Schwann cell membrane [48].

Figure 4 shows representative SMI-312 and S100B staining in healthy (uninjured) sciatic nerve tissue, confirming antibody specificity and staining quality and providing a visual reference point for interpreting the regenerated-tissue images in Section 4. This was used as a basis for quantification and visual analysis of SMI-312 Positive axons and S100B-positive Schwann Cells.

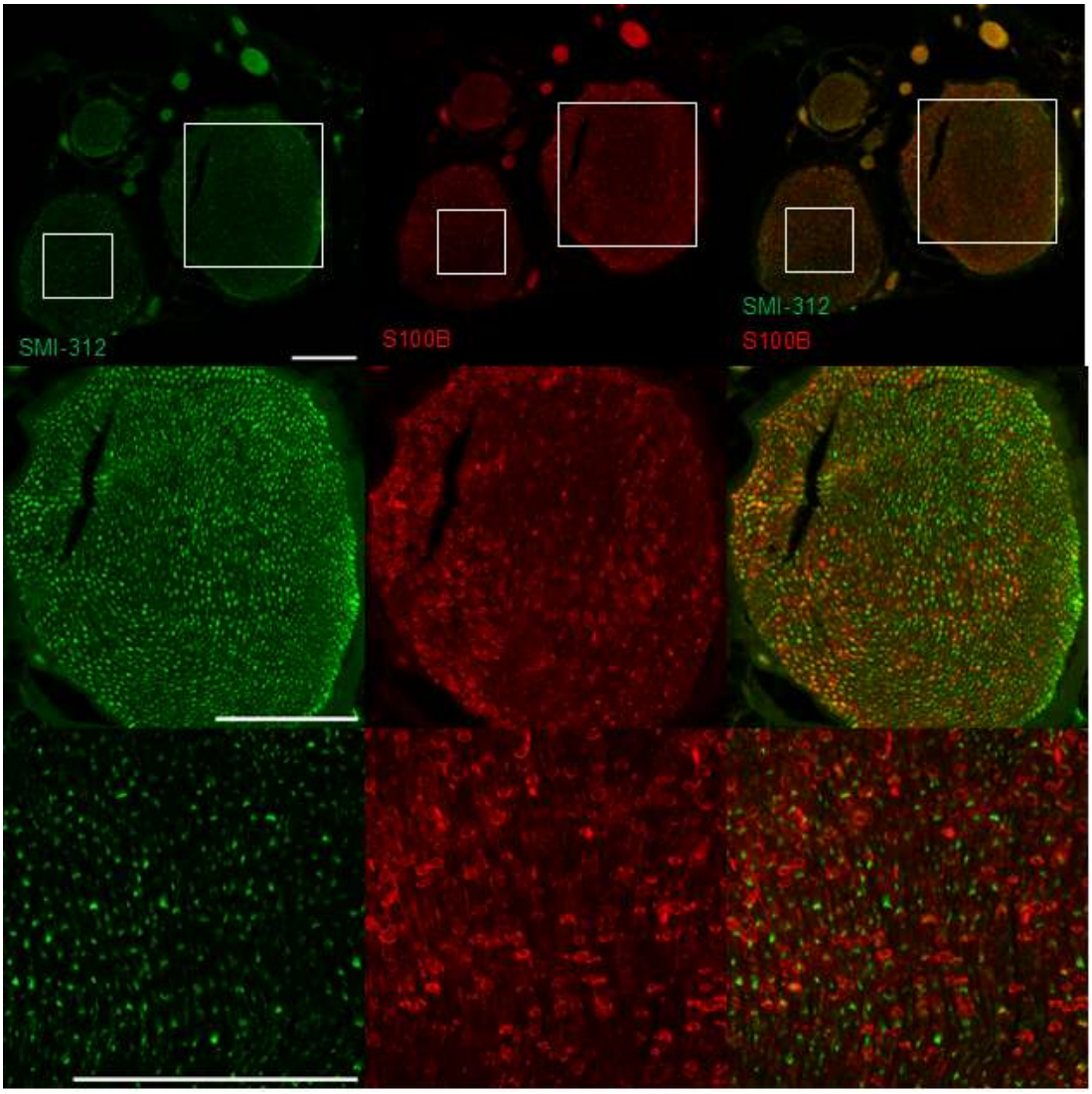

Figure 4: Healthy nerve SMI-312 (green) and S100B (red) staining, with merged image, as an example of immunofluorescent staining quality. White boxes indicate regions shown at higher magnification below the corresponding image. Scale bars represent 250 µm.

Imaging and Quantification

Slides were first imaged in their entirety using an Axio Scan.Z1 automated slide scanner at 10× (408, 488, and 568 nm channels) for documentation purposes only. These images were not used for quantification.

Quantitative imaging used an Olympus BX53 immunofluorescence microscope (4× for initial visualization, 20× for quantification), with image processing and analysis performed in FIJI (v18.0.2). Stitched 20× composite images were generated using the FIJI Stitching plugin. Where automated stitching failed due to low signal or misalignment, images were reconstructed manually using FIJI plugin MosaicJ.

Axons in the proximal nerve were quantified using a RenyiEntropy threshold mask followed by FIJI's particle analysis function. Each thresholded image was then visually cross-checked against the original to identify and add any axons missed by automated counting. Axons in the scaffold and distal nerve were counted manually due to extensive axonal branching, which automated thresholding could not reliably resolve. High resolution images were acquired on an Olympus FV3000 confocal microscope as needed.

Statistical Analysis

Statistical analyses and graph creation were performed using JMP 18.0.2. Quantitative data are presented as mean +/- standard error. Differences between groups were evaluated using an unpaired two-tailed Student’s t-test with statistical significance defined as $p < 0.05$.

RESULTS

Proximal Nerve Quantification and Analysis

Fischer-344 rats underwent a 10 mm sciatic nerve transection and were implanted with a multichannel scaffold, receiving either scaffold-only intervention (n = 18) or scaffold implantation followed by electrical stimulation (6 V, 20 Hz, 110 μs, 10 min; n = 18). Each treatment group was further divided into week 1, week 3, and week 5 cohorts (n = 6 per time point) to characterize the temporal effect of electrical stimulation on axonal growth and end organ weight retention. Representative immunofluorescence images and quantification of axon (SMI-312) and Schwann cell (S100B) markers in the proximal nerve are shown in Figure 5.

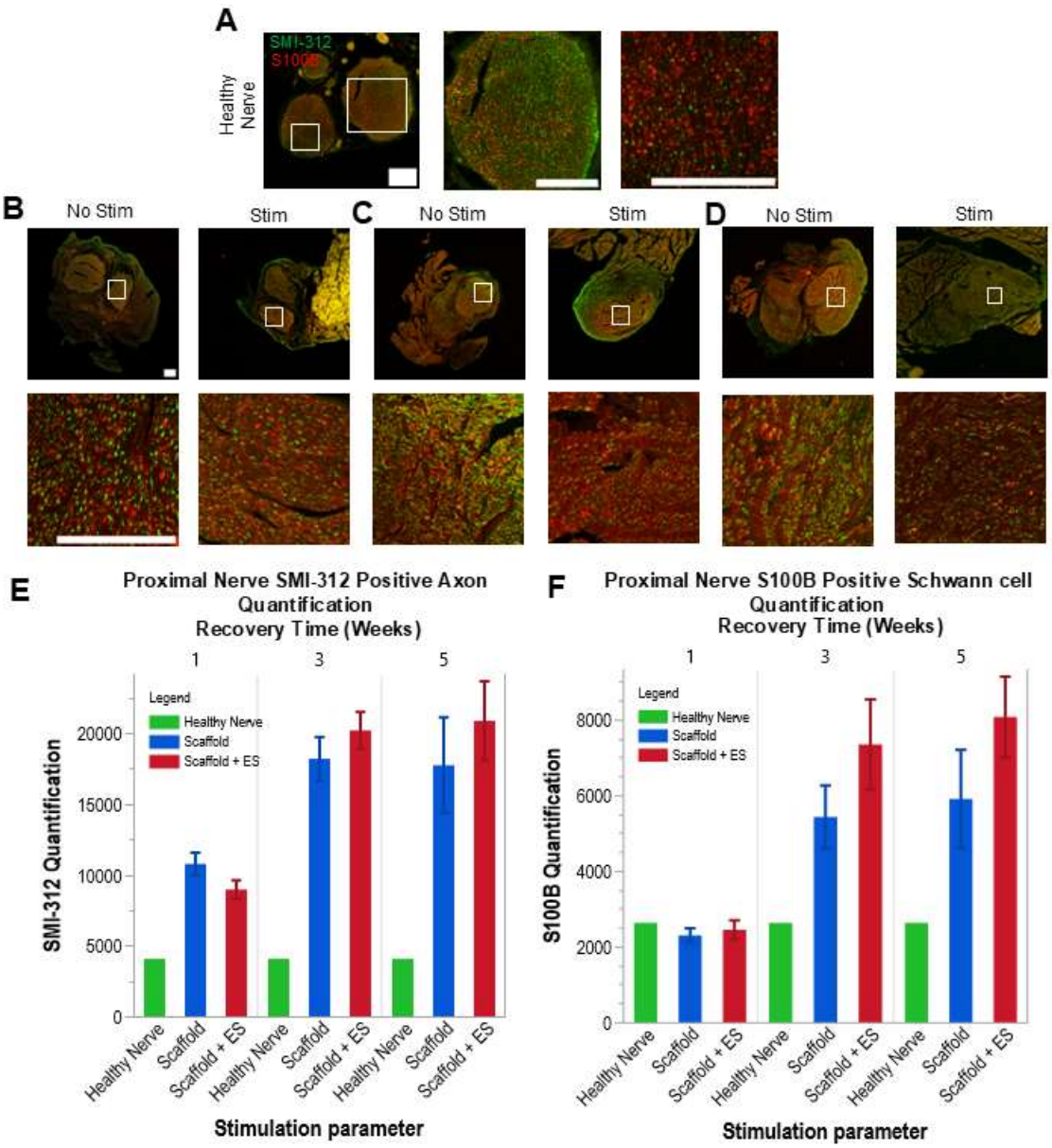

Figure 5: Axon and Schwann cell regeneration in the proximal nerve following injury. (A) Representative cross-sectional image of healthy sciatic nerve tissue stained for neurofilament (SMI-312, green) and Schwann cells (S100B, red), with higher-magnification insets. (B–D) Representative images of regenerated proximal nerve tissue at (B) 1 week, (C) 3 weeks, and (D) 5 weeks post-implantation, for scaffold-only and scaffold+ES groups. White boxes indicate regions shown at higher magnification below the corresponding image; scale bars represent 250 µm. (E) Quantification of SMI-312-positive axons in the proximal nerve at 1, 3, and 5 weeks (week 1 $p = 0.492$, week 3 $p = 0.342$, week 5 $p = 0.111$; no significant difference between groups). (F) Quantification of S100B-positive Schwann cells in the proximal nerve (week 1 $p = 0.649$, week 3 $p = 0.216$, week 5 $p = 0.227$; no significant difference between groups). Data are mean ± standard error; healthy nerve tissue is shown as a representative biological reference and was excluded from statistical comparison. Significance determined by unpaired Student's t-test, $p < 0.05$. Sample size: n = 6/group/time point.

Qualitative comparison of the scaffold-only and scaffold+ES groups showed no visually apparent difference in SMI-312-positive axons or S100B-positive Schwann cells in the proximal nerve (Figure 5 A-D). Healthy (uninjured) nerve tissue was included in the proximal nerve graphs as a biological reference and was excluded from statistical comparison (Figure 5E–F).

Quantification of SMI-312-positive axons showed no significant difference between the scaffold-only and scaffold+ES groups at any time point (Figure 5E). At week 1, axon counts were 10,804 ± 803 and 9,004 ± 644 axons for the scaffold-only and scaffold+ES groups, respectively ($p = 0.492$). At week 3, counts were 18,233 ± 1,529 and 20,237 ± 1,302 axons ($p = 0.342$). At week 5, counts were 17,776 ± 3,381 and 20,908 ± 2,798 axons ($p = 0.111$).

S100B-positive Schwann cell counts in the proximal nerve likewise showed no significant difference between groups at any time point (Figure 5F). With 2,312 ± 189 vs. 2,460 ± 252 cells at week 1 ($p = 0.649$); 5,441 ± 835 vs. 7,361 ± 1,191 cells at week 3 ($p = 0.216$); and 5,921 ± 1,299 vs. 8,086 ± 1,068 cells at week 5 ($p = 0.227$), for scaffold-only and scaffold+ES groups, respectively.

Scaffold Quantification and Analysis

Within the scaffold itself, axon and Schwann cell markers were quantified at the same three time points to assess regeneration inside the conduit (Figure 6).

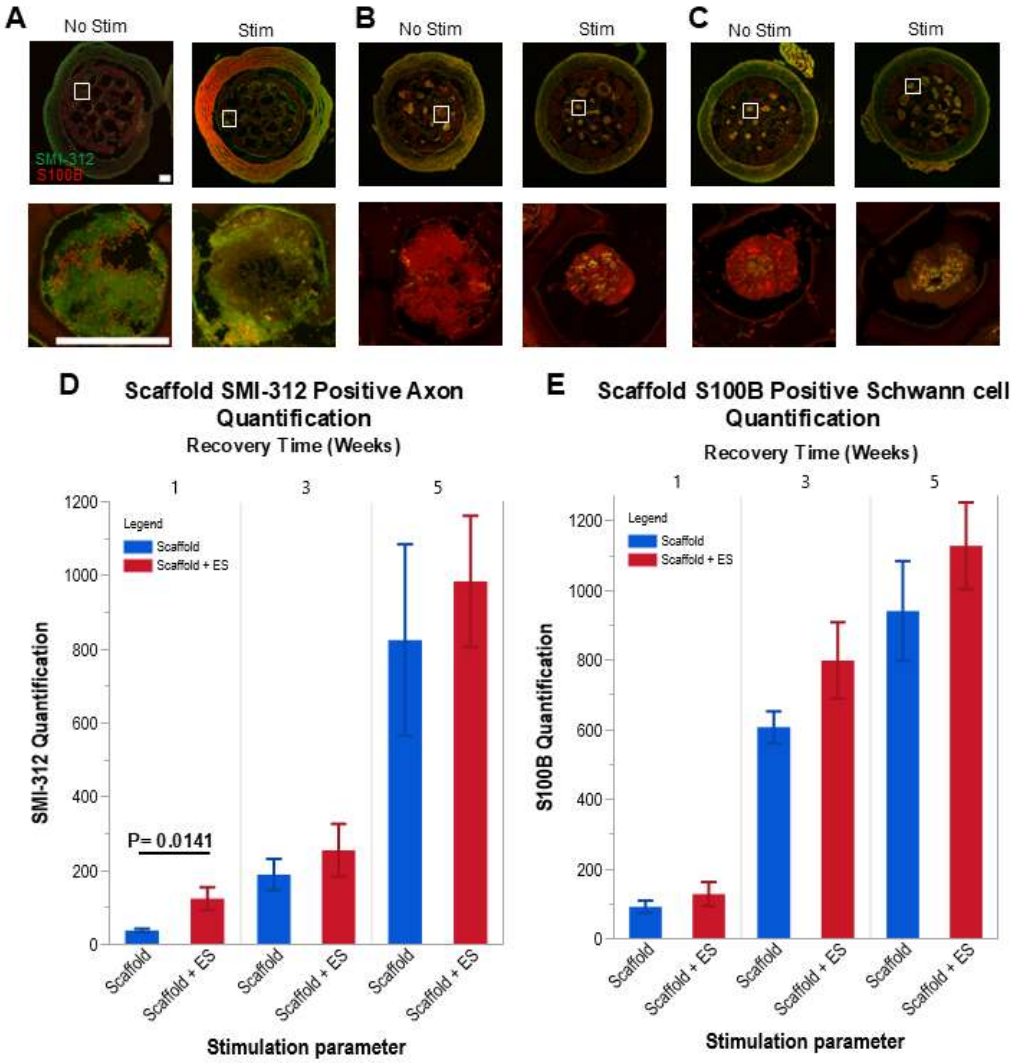

Figure 6: Axon and Schwann cell regeneration within the scaffold. (A–C) Scaffold tissue stained for neurofilament (SMI-312, green) and Schwann cells (S100B, red) at (A) 1 week, (B) 3 weeks, and (C) 5 weeks post-implantation, for scaffold-only and scaffold+ES groups, with higher-magnification insets. Scale bars represent 250 μm. (D) Quantification of SMI-312-positive axons: significant difference at week 1 ($p = 0.014$) and no significant difference at week 3 ($p = 0.448$) or week 5 ($p = 0.624$). (E) Quantification of S100B-positive Schwann cells had no significant difference at week 1 ($p = 0.352$), week 3 ($p = 0.138$), or week 5 ($p = 0.348$). Data are mean ± standard error. Significance determined by unpaired Student's t-test, $p < 0.05$. Sample size: scaffold-only $n = 6$/time point; scaffold+ES $n = 5$ (week 1) and $n = 6$ (weeks 3 and 5).

SMI-312 and S100B were quantified in the early scaffold region at week 1, and in the scaffold midline at weeks 3 and 5. The shift in sampling location reflects the fragility of midline tissue at week 1, which made reliable morphological analysis in that region difficult at this early time point. Incomplete tissue connection between the proximal and distal stumps at week 1 also resulted in the loss of one scaffold sample in the ES group, reducing that time point to $n = 5$ rather than $n = 6$.

SMI-312-positive axon counts differed significantly between groups at week 1, with 38 ± 5 axons in the scaffold-only group versus 124 ± 31 axons in the scaffold+ES group ($p = 0.014$). No significant difference was observed at week 3 (189 ± 43 vs. 255 ± 71 axons, $p = 0.448$) or week 5 (825 ± 260 vs. 984 ± 177 axons, $p = 0.624$) (Figure 6D).

S100B-positive Schwann cell counts showed no significant difference between groups at any time point (Figure 6E): 92 ± 18 vs. 128 ± 35 cells at week 1 ($p = 0.352$); 607 ± 45 vs. 799 ± 110 cells at week 3 ($p = 0.138$); and 941 ± 143 vs. $1{,}129 \pm 128$ cells at week 5 ($p = 0.348$), for scaffold-only and scaffold+ES groups, respectively.

Distal Nerve Quantification and Analysis

Axon and Schwann cell markers were also quantified in the distal nerve, downstream of the scaffold, to evaluate whether regenerating axons reached and repopulated tissue beyond the injury site (Figure 7).

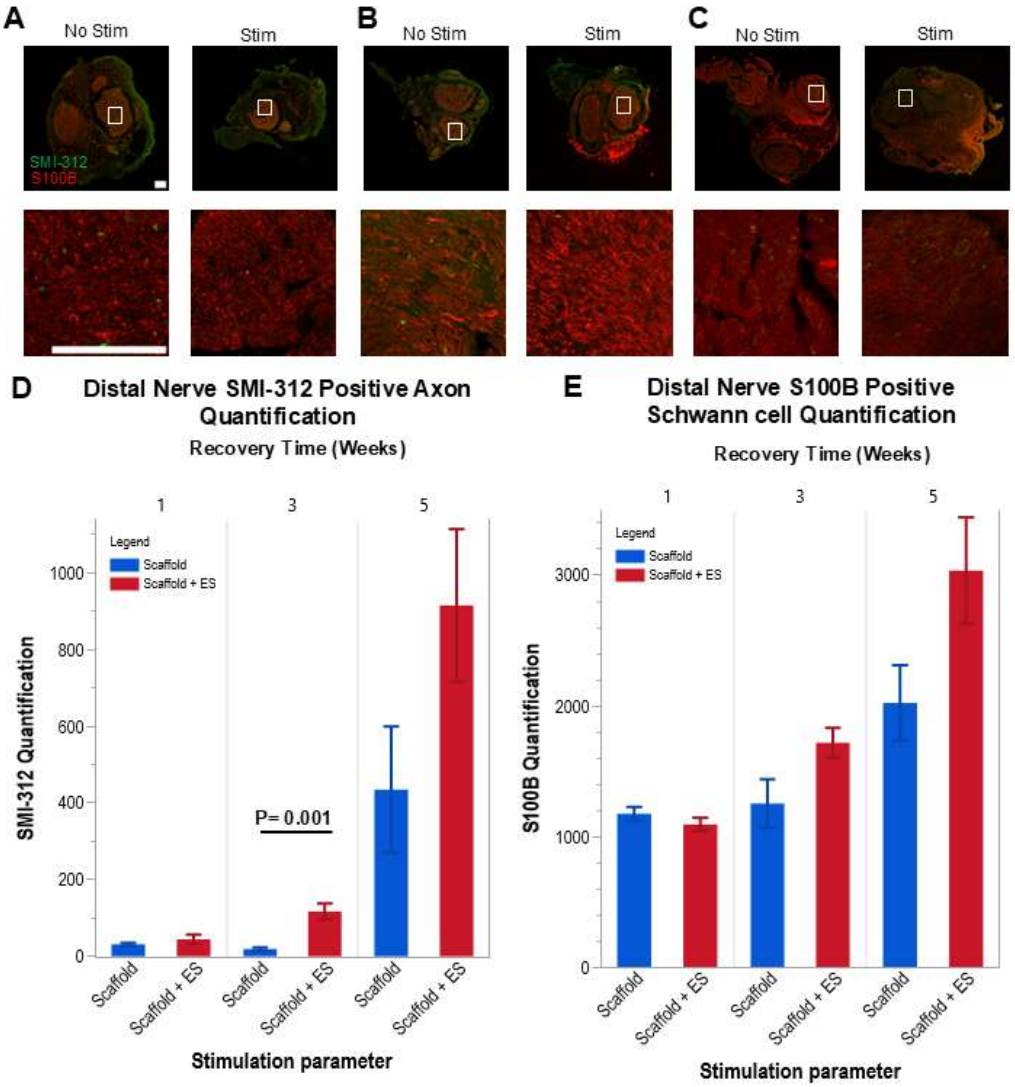

Figure 7: Axon and Schwann cell regeneration in the distal nerve. (A–C) Distal nerve tissue stained for neurofilament (SMI-312, green) and Schwann cells (S100B, red) at (A) 1 week, (B) 3 weeks, and (C) 5 weeks post-implantation, with higher-magnification insets. Scale bars represent 250 µm. (D) Quantification of SMI-312-positive axons: no significant difference at week 1 ($p = 0.330$) or week 5 ($p = 0.093$) but a significant difference at week 3 ($p = 0.001$). (E) Quantification of S100B-positive Schwann cells: no significant difference at week 1 ($p = 0.287$), week 3 ($p = 0.059$), or week 5 ($p = 0.070$). Data are mean ± standard error. Significance determined by unpaired Student's t-test, $p < 0.05$. Sample size: n = 6/group/time point.

SMI-312-positive axon counts in the distal nerve showed no significant difference between groups at week 1 (31 ± 4 vs. 44 ± 12 axons, $p = 0.330$) or week 5 (435 ± 165 vs. 915 ± 199 axons, $p = 0.093$), but differed significantly at week 3 (19 ± 4 vs. 117 ± 21 axons, $p = 0.001$) (Figure 7D). Although the week 5 difference did not reach statistical significance, the scaffold+ES group showed nearly double the mean axon count of the scaffold-only group, suggesting a possible trend toward greater distal regeneration with stimulation.

S100B-positive Schwann cell counts also showed no significant difference between groups at any distal nerve time point (Figure 7E). With a count of 1,176 ± 52 vs. 1,094 ± 52 cells at week 1 ($p = 0.287$), 1,255 ± 186 vs. 1,719 ± 113 cells at week 3 ($p = 0.059$), and 2,023 ± 288 vs. 3,035 ± 407 cells at week 5 ($p = 0.070$), for scaffold-only and scaffold+ES groups respectively. Although not statistically significant, Schwann cell counts were consistently higher in the ES group at weeks 3 and 5, with p-values approaching the significance threshold of $p < 0.05$ for statistical significance suggesting a possible ES-associated increase in Schwann cell number that this study was not powered to detect.

Overall, quantification of SMI-312 and S100B in the distal nerve did not reach statistical significance at every time point, but the consistent direction of the S100B trend at weeks 3 and 5 may reflect a true underlying effect that a larger sample size could resolve.

Left Gastrocnemius Muscle Retention and Analysis

Left gastrocnemius muscle weight was measured as an indicator of downstream muscle reinnervation, since prolonged denervation leads to muscle atrophy and weight loss (Figure 8).

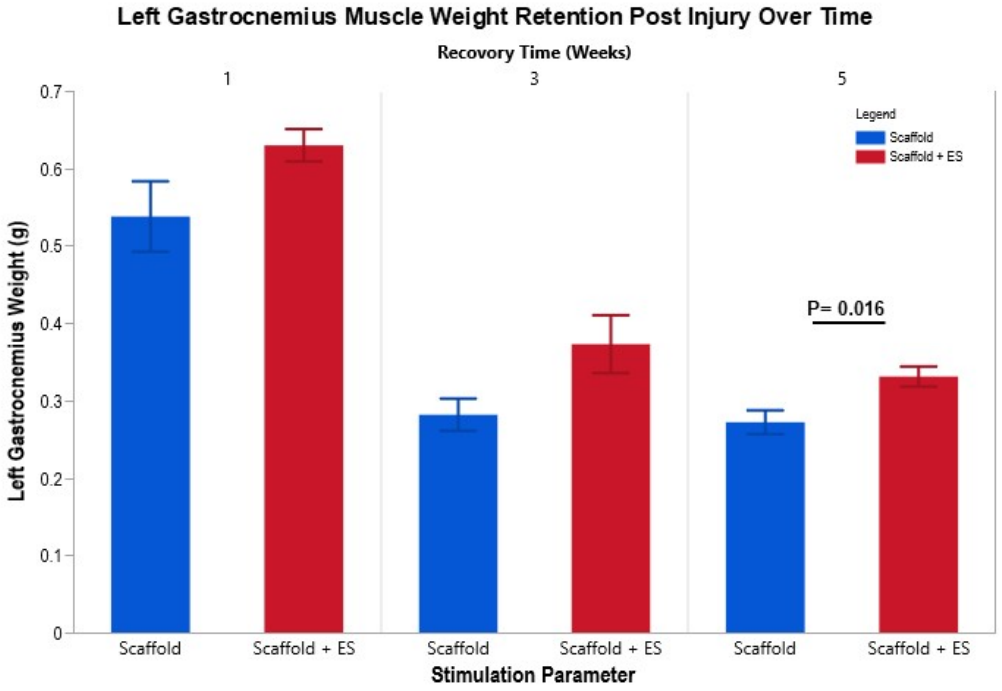

Figure 8: Left gastrocnemius muscle weight retention following sciatic nerve repair. Left gastrocnemius muscle weight was measured at 1, 3, and 5 weeks post-implantation. No significant difference was found at week 1 ($p = 0.109$) or week 3 ($p = 0.067$); a significant difference was found at week 5 ($p = 0.016$). Bars represent mean ± standard error. Statistical analysis performed using an unpaired Student's t-test, $p < 0.05$. Sample size: n = 6/group/time point.

Gastrocnemius muscle weight was consistently higher in the scaffold+ES group relative to the scaffold-only group across all time points (Figure 8). At week 1, mean muscle weight was 0.539 ± 0.046 g in the scaffold-only group versus 0.631 ± 0.021 g in the scaffold+ES group ($p = 0.109$). At week 3, weights were 0.282 ± 0.021 g versus 0.373 ± 0.037 g ($p = 0.067$), approaching but not reaching statistical significance. At week 5, the difference reached statistical significance, with mean weights of 0.272 ± 0.015 g and 0.332 ± 0.013 g for the scaffold-only and scaffold+ES groups, respectively ($p = 0.016$).

Although the week 1 and week 3 differences were not statistically significant, the consistently higher mean weight in the ES group, combined with a p-value that decreased progressively from week 1 to week 5, is consistent with electrical stimulation reducing end-organ degeneration over time.

DISCUSSION

This study examined whether combining brief electrical stimulation (ES) (10min, 6 V, 20 Hz, 110 μs pulse) with biomimetic multichannel nerve guidance conduits/scaffolds (NGC) changes axonal regeneration and Schwann cell response following sciatic nerve transection, relative to scaffold implantation alone. Compared to scaffold-only treatment, scaffold+ES significantly increased axon counts within the scaffold at week 1, in the distal nerve at week 3, and significantly increased gastrocnemius muscle weight at week 5, a pattern suggesting that ES produces a temporally progressive regenerative benefit, leading to faster recovery, rather than a uniform increase across all time points and tissue regions (Figure 9).

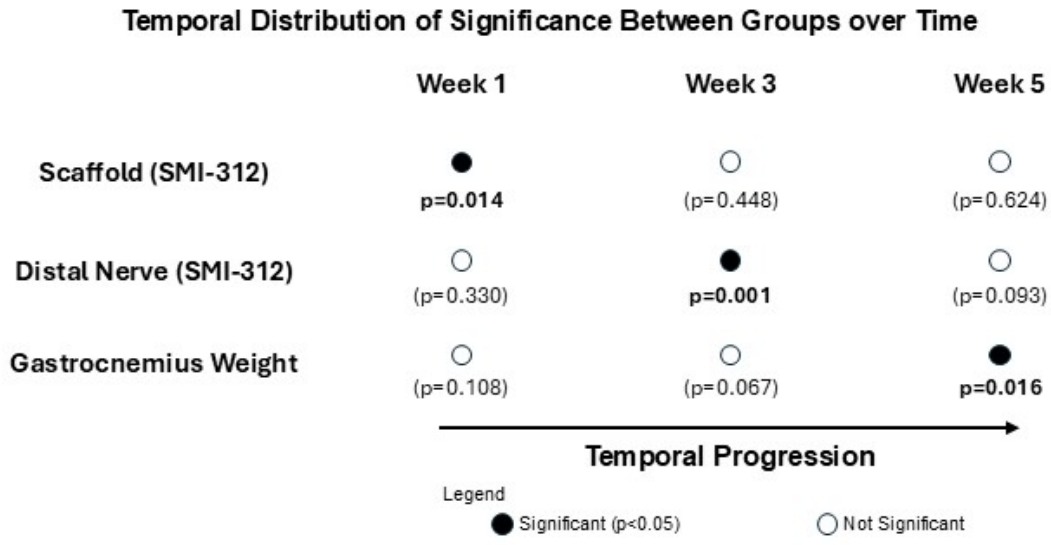

Figure 9: Temporal distribution of statistically significant difference in quantified endpoints, compared between stimulation and no stimulation treatment over time. Comparisons between the scaffold + electrical stimulation and scaffold-only groups are shown across Week 1, Week 3, and Week 5 for SMI-312-positive axons within the scaffold and distal nerve, as well as gastrocnemius muscle weight. Filled circles indicate statistically significant differences ($p < 0.05$), while open circles indicate non-significant comparisons. Significant differences were observed in the scaffold at Week 1 ($p = 0.014$), the distal nerve at Week 3 ($p = 0.001$), and gastrocnemius weight at Week 5 ($p = 0.016$), when animals were treated with scaffolds+ES. No significant differences were observed in the remaining comparisons, including the Week 5 distal nerve ($p = 0.093$). The distribution of significant findings demonstrates a temporal progression from the scaffold to the distal nerve and, subsequently, to gastrocnemius muscle weight.

By week 3, axon counts within the scaffold no longer differed between groups, suggesting the scaffold-only group had largely caught up to the ES group within the conduit itself. By week 5, axon counts in the distal nerve also converged, though the ES group's mean remained nearly double that of the scaffold-only group.

Quantification of S100B, a calcium-binding protein broadly expressed by Schwann cells regardless of myelination state or regenerative phenotype [48, 49], reflects total Schwann cell number rather than a specific subpopulation or degree of myelination at a given time point. S100B counts did not differ significantly between groups at any time point or tissue region however, in the distal nerve, S100B-positive counts remained elevated. Particularly in the ES group at week 3 ($p = 0.059$) and week 5 ($p = 0.070$), where p-values are close to, but not below, the $p < 0.05$ threshold (Figure 7E). This pattern may reflect earlier axon reconnection in the ES group, as Schwann cells that make earlier contact with regenerating axons may be less likely to undergo apoptosis associated with prolonged denervation. It may also reflect upregulation of S100B during active regeneration [49] rather than a true change in cell number. Distinguishing between these possibilities would require additional markers of Schwann cell repair phenotype, such as c-Jun, Sox2, or p75-NTR. Even without a statistically significant difference, the consistent direction of this trend is compatible with a possible positive effect of ES on Schwann cell maturation, migration, or phenotype, and further study in this area is warranted.

Gastrocnemius muscle weight was assessed as an indicator of end organ reinnervation, since muscle retention is associated with better functional recovery. [50]. Muscle weight increased progressively in the scaffold+ES group, reaching statistical significance by week 5 ($p = 0.016$) (Figure 8), consistent with prior reports that ES limits early end organ degeneration. In gap injuries, muscle degeneration typically proceeds quickly in the absence of axon input [25]. The

progressively higher gastrocnemius weight observed here suggests that ES slowed this degeneration, potentially supporting better functional outcomes as axons continued to reach the end organ. Direct analysis of motor neuron reinnervation, along with long term behavioral studies, would be needed to confirm whether this translates into improved functional recovery.

Taken together, the slower muscle degeneration and accelerated axon progression observed with biomimetic scaffold intervention + ES support the hypothesis that brief electrical stimulation improves axon regeneration and end organ retention. The findings suggest that rather than producing a uniform increase in axonal regeneration at every tissue region and time point, scaffold + ES produced a spatially and temporally distributed pattern of treatment. The pattern is represented in the earliest significant finding in the study, occurring at week 1 in the scaffold, followed by week 3 in the distal nerve and finally in week 5 in the gastrocnemius muscle retention weight.

This progression is particularly important in the context of gap peripheral nerve injury. A successful repair strategy must not only promote axonal growth but facilitate the progression of regenerating axons across the injury and toward the distal stump for eventual end organ reintervention [2]. The present findings are consistent with the possibility that ES provides an early biological stimulus for regeneration, while multichannel scaffold provides the physical structure necessary to guide those axons across the injury. The combination may therefore provide complementary benefits that are not achieved as effectively through either regenerative stimulation or structural guidance alone.

Several extensions of this work could strengthen these findings. Longitudinal imaging of SMI-312-positive axons would clarify not only how many axons regenerate at each time point, but

how far they extend along the scaffold. Further characterization of Schwann cell phenotype in response to ES for instance, using c-Jun as a marker of the pro-regenerative state could help clarify the mechanism underlying the S100B trend observed here. Direct assessment of motor neuron reinnervation would also strengthen interpretation of the muscle weight data, since weight alone cannot confirm functional reinnervation. Longterm functional studies are similarly needed to determine whether ES produces a lasting improvement in outcome. Finally, this study did not include an a priori power analysis to determine time point sample sizes, given the limited prior literature on combining biomimetic multichannel scaffolds with ES. The near significant findings reported here (e.g., distal nerve week 5, $p = 0.093$; distal S100B weeks 3 and 5) suggest that a larger sample size might resolve some of these trends as statistically significant, and should inform the design of future, more definitive studies.

This exploratory study provides early evidence that electrical stimulation, when combined with a biomimetic multichannel nerve guidance scaffold, produces a temporally progressive regenerative benefit through an increase in axon counts within the scaffold at week 1, increased axon counts in the distal nerve at week 3, and increased gastrocnemius muscle weight by week 5. As the field continues to explore alternatives to autograft repair for long-gap nerve injuries, these findings support further investigation of ES as a strategy to improve functional outcomes.

CONCLUSIONS AND FUTURE DIRECTIONS

Axonal regeneration following peripheral nerve injury remains a major clinical challenge, driven primarily by poor axonal directionality and progressive end organ degeneration that together limit functional recovery. In complete transection or severe intraneural disruption, spontaneous recovery is essentially impossible without surgical intervention [51] Biomimetic multichannel scaffolds have emerged as a promising alternative to the autograft gold standard, offering enhanced axonal guidance with regenerative efficacy comparable to autograft. However, in gap injuries, axonal reconnection to the distal stump and the eventual reinnervation of the end organ remains slow, limited by the intrinsically gradual rate of peripheral axon growth. Brief electrical stimulation (ES) has previously been explored as a strategy to accelerate regeneration, but its translation into clinical practice has been limited by its tendency to cause axonal misdirection. This study compared nerve regeneration and end organ retention between scaffold+ES and scaffold-only treatment to clarify whether combining the two addresses this limitation.

Quantification of SMI-312 showed that combining ES with a biomimetic multichannel scaffold produced a temporally progressive pattern of regeneration. With greater axonal growth within the scaffold at week 1, greater axonal regeneration in the distal nerve at week 3, and a difference approaching significance in the distal nerve at week 5. These findings suggest that ES accelerated the rate of axonal regeneration, allowing axons to reach the distal nerve earlier than with scaffold-only treatment. Quantification of S100B, though not statistically significant, showed a consistent increase in Schwann cell counts at weeks 1, 3, and 5 in the ES group, suggesting a possible acceleration of Schwann cell maturation and a reduction in denervation-associated cell loss. Gastrocnemius muscle weight followed a similar pattern, with the ES group showing higher

average retention at every time point and a statistically significant difference by week 5. Together, these findings suggest that biomimetic multichannel scaffolds provide a temporal regenerative benefit of electrical stimulation in peripheral nerve repair and end organ retention.

Future work combining ES with biomimetic multichannel scaffolds could be strengthened by several additions. Analysis of c-Jun, a regulator of the Schwann cell pro-regenerative state, would help clarify the mechanism underlying the Schwann cell trends observed here. Prior work has shown that ES upregulates c-Jun expression in Schwann cells in vivo [52]. Development of an electrically conductive multichannel scaffold could also improve the delivery of stimulation throughout the injury site, since stimulation at the distal side of the injury has separately been shown to improve end-organ retention and function [53]. The near-significant findings reported here suggest that a larger sample size per group may be needed to confirm whether these trends reach statistical significance. Finally, incorporating long-term functional recovery assessments would better support the interpretation that enhanced end-organ retention translates into meaningful functional recovery after multichannel scaffold implantation with electrical stimulation.

REFERENCES

[1] Al-Majed, A. A., Neumann, C. M., Brushart, T. M., & Gordon, T. (2000). Brief Electrical Stimulation Promotes the Speed and Accuracy of Motor Axonal Regeneration. *Journal of Neuroscience, 20*(7), 2602–2608. https://doi.org/10.1523/JNEUROSCI.20-07-02602.2000

[2] Gordon, T. (2020). Peripheral Nerve Regeneration and Muscle Reinnervation. *International Journal of Molecular Sciences, 21*(22), 8652. https://doi.org/10.3390/ijms21228652

[3] Stoll, G., & Müller, H. W. (2006). Nerve Injury, Axonal Degeneration and Neural Regeneration: Basic Insights. *Brain Pathology, 9*(2), 313–325. https://doi.org/10.1111/j.1750-3639.1999.tb00229.x

[4] Ni, L., Yao, Z., Zhao, Y., Zhang, T., Wang, J., Li, S., & Chen, Z. (2023). Electrical stimulation therapy for peripheral nerve injury. *Frontiers in Neurology, 14*. https://doi.org/10.3389/fneur.2023.1081458

[5] Udina, E., Furey, M., Busch, S., Silver, J., Gordon, T., & Fouad, K. (2008). Electrical stimulation of intact peripheral sensory axons in rats promotes outgrowth of their central projections. *Experimental Neurology, 210*(1), 238–247. https://doi.org/10.1016/j.expneurol.2007.11.007

[6] Juckett, L., Saffari, T. M., Ormseth, B., Senger, J.-L., & Moore, A. M. (2022). The Effect of Electrical Stimulation on Nerve Regeneration Following Peripheral Nerve Injury. *Biomolecules, 12*(12), 1856. https://doi.org/10.3390/biom12121856

[7] Koffler, J., Zhu, W., Qu, X., Platoshyn, O., Dulin, J. N., Brock, J., Graham, L., Lu, P., Sakamoto, J., Marsala, M., Chen, S., & Tuszynski, M. H. (2019). Biomimetic 3D-printed scaffolds for spinal cord injury repair. *Nature Medicine, 25*(2), 263–269. https://doi.org/10.1038/s41591-018-0296-z

[8] Koffler, J., Sinopoulou, E., Lazarovits, I., Alexander, M. W. A., Salcido, A., Pawalelec, K., Abrams, R., Sakamoto, K., & Tuszynski, M. H. (2026). Multichannel, Biomimetic Scaffolds Improve Functional Connectivity Following Traumatic Long-Gap Peripheral Nerve Injury. *Nature Communications*. Accepted.

[9] Mankavi, F., Ibrahim, R., & Wang, H. (2023). Advances in Biomimetic Nerve Guidance Conduits for Peripheral Nerve Regeneration. *Nanomaterials, 13*(18), 2528. https://doi.org/10.3390/nano13182528

[10] Choi, Y., & Noh, H. (Moses). (2016). Peripheral nerve regeneration monitoring using multilayer microchannel scaffolds. *Neural Regeneration Research, 11*(3), 422–423. https://doi.org/10.4103/1673-5374.179052

[11] Pedrosa, S. S., Caseiro, A. R., & Maurício, J. D. S. and A. C. (2017). Scaffolds for Peripheral Nerve Regeneration, the Importance of In Vitro and In Vivo Studies for the Development of Cell-Based Therapies and Biomaterials: State of the Art. In *Scaffolds in Tissue Engineering—Materials, Technologies and Clinical Applications*. IntechOpen. https://doi.org/10.5772/intechopen.69540

[12] Muzio, M. R., Fakoya, A. O., & Cascella, M. (2026). Histology, Axon. In *StatPearls*. StatPearls Publishing. http://www.ncbi.nlm.nih.gov/books/NBK554388/

[13] Fallon, M., & Tadi, P. (2026). Histology, Schwann Cells. In *StatPearls*. StatPearls Publishing. http://www.ncbi.nlm.nih.gov/books/NBK544316/

[14] Salzer, J. L., & Zalc, B. (2016). Myelination. *Current Biology, 26*(20), R971–R975. https://doi.org/10.1016/j.cub.2016.07.074

[15] Parkinson, D. B., Bhaskaran, A., Arthur-Farraj, P., Noon, L. A., Woodhoo, A., Lloyd, A. C., Feltri, M. L., Wrabetz, L., Behrens, A., Mirsky, R., & Jessen, K. R. (2008). C-Jun is a negative regulator of myelination. *The Journal of Cell Biology, 181*(4), 625–637. https://doi.org/10.1083/jcb.200803013

[16] Chhabra, A., Ahlawat, S., Belzberg, A., & Andreseik, G. (2014). Peripheral nerve injury grading simplified on MR neurography: As referenced to Seddon and Sunderland classifications. *The Indian Journal of Radiology & Imaging, 24*, 217–224. https://doi.org/10.4103/0971-3026.137025

[17] Seddon, H. J. (1942). A Classification of Nerve Injuries. https://doi.org/10.1136/bmj.2.4260.237

[18] Sunderland, S. (1951). A Classification of Peripheral Nerve Injuries Producing Loss of Function. *Brain, 74*(4), 491–516. https://doi.org/10.1093/brain/74.4.491

[19] Eder, M., Schulte-Mattler, W., & Pöschl, P. (2017). Neurographic course of Wallerian degeneration after human peripheral nerve injury. *Muscle & Nerve, 56*(2), 247–252. https://doi.org/10.1002/mus.25489

[20] Conforti, L., Gilley, J., & Coleman, M. P. (2014). Wallerian degeneration: An emerging axon death pathway linking injury and disease. *Nature Reviews Neuroscience, 15*(6), 394–409. https://doi.org/10.1038/nrn3680

[21] Tian, R., Zhou, Y., Ren, Y., Zhang, Y., & Tang, W. (2025). Wallerian degeneration: From mechanism to disease to imaging. *Heliyon, 11*(1), e40729. https://doi.org/10.1016/j.heliyon.2024.e40729

[22] Pandey, S., & Mudgal, J. (2022). A Review on the Role of Endogenous Neurotrophins and Schwann Cells in Axonal Regeneration. *Journal of Neuroimmune Pharmacology, 17*(3), 398–408. https://doi.org/10.1007/s11481-021-10034-3

[23] Wan, T., Zhang, F.-S., Qin, M.-Y., Jiang, H.-R., Zhang, M., Qu, Y., Wang, Y.-L., & Zhang, P.-X. (2024). Growth factors: Bioactive macromolecular drugs for peripheral nerve injury treatment – Molecular mechanisms and delivery platforms. *Biomedicine & Pharmacotherapy, 170*, 116024. https://doi.org/10.1016/j.biopha.2023.116024

[24] Fuentes-Flores, A., Geronimo-Olvera, C., Girardi, K., Necuñir-Ibarra, D., Patel, S. K., Bons, J., Wright, M. C., Geschwind, D., Hoke, A., Gomez-Sanchez, J. A., Schilling, B., Rebolledo, D. L., Campisi, J., & Court, F. A. (2023). Senescent Schwann cells induced by aging and chronic denervation impair axonal regeneration following peripheral nerve injury. *EMBO Molecular Medicine, 15*(12), e17907. https://doi.org/10.15252/emmm.202317907

[25] Burrell, J. C., Ali, Z. S., Zager, E. L., Rosen, J. M., Tatarchuk, M. M., & Cullen, D. K. (2025). Engineering the Future of Restorative Clinical Peripheral Nerve Surgery. *Advanced Healthcare Materials, 14*(20), 2404293. https://doi.org/10.1002/adhm.202404293

[26] Ciaramitaro, P., Mondelli, M., Logullo, F., Grimaldi, S., Battiston, B., Sard, A., Scarinzi, C., Migliaretti, G., Faccani, G., Cocito, D., & Neuropathies, on behalf of the Italian Network for Traumatic. (2010). Traumatic peripheral nerve injuries: Epidemiological findings, neuropathic pain and quality of life in 158 patients. *Journal of the Peripheral Nervous System, 15*(2), 120–127. https://doi.org/10.1111/j.1529-8027.2010.00260.x

[27] de Ruiter, G. C. W., Spinner, R. J., Yaszemski, M. J., Windebank, A. J., & Malessy, M. J. A. (2009). Nerve Tubes for Peripheral Nerve Repair. *Neurosurgery Clinics of North America, 20*(1), 91–105. https://doi.org/10.1016/j.nec.2008.08.001

[28] Li, Y., Ma, Z., Ren, Y., Lu, D., Li, T., Li, W., Wang, J., Ma, H., & Zhao, J. (2021). Tissue Engineering Strategies for Peripheral Nerve Regeneration. *Frontiers in Neurology, 12*. https://doi.org/10.3389/fneur.2021.768267

[29] Muheremu, A., & Ao, Q. (2015). Past, Present, and Future of Nerve Conduits in the Treatment of Peripheral Nerve Injury. *BioMed Research International, 2015*, 237507. https://doi.org/10.1155/2015/237507

[30] Yu, L., Bennett, C. J., Lin, C.-H., Yan, S., & Yang, J. (2024). Scaffold design considerations for peripheral nerve regeneration. *Journal of Neural Engineering, 21*(4). https://doi.org/10.1088/1741-2552/ad628d

[31] Foy, C. A., & Kuffler, D. P. (2025). Limitations to clinically restoring meaningful peripheral nerve function across gaps and overcoming them. *Experimental Biology and Medicine, 250*, 10566. https://doi.org/10.3389/ebm.2025.10566

[32] Johnson, P. J., Wood, M. D., Moore, A. M., & Mackinnon, S. E. (2013). Tissue engineered constructs for peripheral nerve surgery. *European Surgery: ACA: Acta Chirurgica Austriaca, 45*(3). https://doi.org/10.1007/s10353-013-0205-0

[33] Messana, F., Lucchetta, G., Bassetto, F., & Tiengo, C. (2024). Comparative evaluation of neurotubules and autologous nerve grafts for peripheral nerve repair: A retrospective case series. *Plastic Reconstructive and Regenerative Surgery*, 32–38. https://doi.org/10.57604/PRRS-445

[34] Moore, A. M., Kasukurthi, R., Magill, C. K., Farhadi, H. F., Borschel, G. H., & Mackinnon, S. E. (2009). Limitations of Conduits in Peripheral Nerve Repairs. *Hand (New York, N.Y.), 4*(2), 180–186. https://doi.org/10.1007/s11552-008-9158-3

[35] Pawelec, K. M., Hix, J., Shapiro, E. M., & Sakamoto, J. (2019). The mechanics of scaling-up multichannel scaffold technology for clinical nerve repair. *Journal of the Mechanical Behavior of Biomedical Materials, 91*, 247–254. https://doi.org/10.1016/j.jmbbm.2018.12.016

[36] Gordon, T. (2016). Electrical Stimulation to Enhance Axon Regeneration After Peripheral Nerve Injuries in Animal Models and Humans. *Neurotherapeutics, 13*(2), 295–310. https://doi.org/10.1007/s13311-015-0415-1

[37] Koppes, A. N., Nordberg, A. L., Paolillo, G. M., Goodsell, N. M., Darwish, H. A., Zhang, L., & Thompson, D. M. (2014). Electrical Stimulation of Schwann Cells Promotes Sustained Increases in Neurite Outgrowth. *Tissue Engineering. Part A, 20*(3–4), 494–506. https://doi.org/10.1089/ten.tea.2013.0012

[38] Gordon, T. (2024). Brief Electrical Stimulation Promotes Recovery after Surgical Repair of Injured Peripheral Nerves. *International Journal of Molecular Sciences, 25*(1), 665. https://doi.org/10.3390/ijms25010665

[39] Roh, J., Schellhardt, L., Keane, G. C., Hunter, D. A., Moore, A. M., Snyder-Warwick, A. K., Mackinnon, S. E., & Wood, M. D. (2022). Short-Duration, Pulsatile, Electrical Stimulation Therapy Accelerates Axon Regeneration and Recovery Following Tibial Nerve Injury and Repair in Rats. *Plastic and Reconstructive Surgery, 149*(4), 681e–690e. https://doi.org/10.1097/PRS.0000000000008924

[40] Saffari, T. M., Walker, E. R., Pet, M. A., & Moore, A. M. (2024). Brief Intraoperative Electrical Stimulation to Enhance Nerve Regeneration. *Plastic and Reconstructive Surgery Global Open, 12*(4), e5730. https://doi.org/10.1097/GOX.0000000000005730

[41] Aglah, C., Gordon, T., & Posse De Chaves, E. I. (2008). cAMP promotes neurite outgrowth and extension through protein kinase A but independently of Erk activation in cultured rat motoneurons. *Neuropharmacology, 55*(1), 8–17. https://doi.org/10.1016/j.neuropharm.2008.04.005

[42] Willand, M. P., Nguyen, M.-A., Borschel, G. H., & Gordon, T. (2016). Electrical Stimulation to Promote Peripheral Nerve Regeneration. *Neurorehabilitation and Neural Repair, 30*(5), 490–496. https://doi.org/10.1177/1545968315604399

[43] Gordon, T., & English, A. W. (2016). Strategies to promote peripheral nerve regeneration: Electrical stimulation and/or exercise. *The European Journal of Neuroscience, 43*(3), 336–350. https://doi.org/10.1111/ejn.13005

[44] English, A. W. (2005). Enhancing axon regeneration in peripheral nerves also increases functionally inappropriate reinnervation of targets. *Journal of Comparative Neurology, 490*(4), 427–441. https://doi.org/10.1002/cne.20678

[45] Hamilton, S. K., Hinkle, M. L., Nicolini, J., Rambo, L. N., Rexwinkle, A. M., Rose, S. J., Sabatier, M. J., Backus, D., & English, A. W. (2011). Misdirection of Regenerating Axons and Functional Recovery Following Sciatic Nerve Injury in Rats. *The Journal of Comparative Neurology, 519*(1), 21–33. https://doi.org/10.1002/cne.22446

[46] *Purified anti-Neurofilament Marker (pan axonal, cocktail)*. (n.d.). BioLegend. Retrieved August 13, 2026, from https://www.biolegend.com/en-gb/products/purified-anti-neurofilament-marker-pan-axonal-cocktail-12811?GroupID=BLG15643

[47] Ulfig, N., Nickel, J., & Bohl, J. (1998). Monoclonal antibodies SMI 311 and SMI 312 as tools to investigate the maturation of nerve cells and axonal patterns in human fetal brain. *Cell and Tissue Research, 291*(3), 433–443. https://doi.org/10.1007/s004410051013

[48] *Schwann cell markers throughout development*. (n.d.). Abcam. Retrieved August 13, 2026, from https://www.abcam.com/en-us/technical-resources/research-areas/marker-guides/schwann-cell-markers

[49] Sorci, G., Riuzzi, F., Arcuri, C., Tubaro, C., Bianchi, R., Giambanco, I., & Donato, R. (2013). S100B protein in tissue development, repair and regeneration. *World Journal of Biological Chemistry, 4*(1), 1–12. https://doi.org/10.4331/wjbc.v4.i1.1

[50] Mohammadi, R., & Mahmoodi, H. (2013). Improvement of peripheral nerve regeneration following nerve repair by silicone tube filled with curcumin: A preliminary study in the rat model. *International Journal of Surgery, 11*(9), 819–825. https://doi.org/10.1016/j.ijsu.2013.08.011

[51] Baek, A., & Isaacs, J. (2024). Management of “Long” Nerve Gaps. *Journal of Hand Surgery Global Online, 6*(5), 685–690. https://doi.org/10.1016/j.jhsg.2024.01.012

[52] Jessen, K. R., & Mirsky, R. (2016). The repair Schwann cell and its function in regenerating nerves. *The Journal of Physiology, 594*(13), 3521–3531. https://doi.org/10.1113/JP270874

[53] Johnson, J. M., Lama, C., Singh, M., Piana, L. E., & Gil, J. A. (2025). Electrical stimulation in peripheral nerve injuries: A review of current literature. *Hand Surgery and Rehabilitation, 44*(6), 102525. https://doi.org/10.1016/j.hansur.2025.102525